

# The Influence of Isotropic Compression Stiffness on Ground Deformation Induced by Shallow Tunnels

Felipe Paiva Magalhães Vitali

Ph.D. student, Department of Geotechnical Engineering, Engineering School of São Carlos, University of São Paulo, São Carlos, SP, Brazil. [felipe.vitali@usp.br](mailto:felipe.vitali@usp.br)

Oswaldo Paiva Magalhães Vitali

Assistant Professor. Department of Civil, Environmental and Construction Engineering, University of Hawaii at Manoa, HI, United States. [opmv@hawaii.edu](mailto:opmv@hawaii.edu)

Tarcisio Barreto Celestino

Professor, Department of Geotechnical Engineering, Engineering School of São Carlos, University of São Paulo, São Carlos, SP, Brazil. [tbcelest@usp.br](mailto:tbcelest@usp.br)

**ABSTRACT:** Tunnel construction in highly compressible soils, such as porous clays, may induce large ground deformations, potentially damaging buildings and existing infrastructure. Typically, these soils exhibit significant volumetric contraction, leading to a complex distribution of displacements around the tunnel. Notable examples of tunnels in porous clays are the Metro tunnels in Brasília and the Paraíso tunnel in São Paulo. Given the complexity of the problem, the use of numerical modeling with sophisticated constitutive models becomes imperative. The Hardening Soil Model, a well-known constitutive model for soils, accurately reproduces the behavior of various soil types. Its parameters can be easily derived from laboratory tests or estimated from in-situ testing. For this reason, this constitutive model is widely used in Geotechnical Engineering practice. In this paper, the Paraíso tunnel is analyzed using a 2D plane strain Finite Element Method (FEM) model using the tunnel volume loss control technique. The Hardening Soil Model was calibrated using compression and extension triaxial tests on undisturbed samples of the residual porous clays of São Paulo. A good match was found between the numerical model results and field data when the tunnel volume loss equals 1.25%. Then, a sensitivity analysis was conducted to assess the influence of the 1D-compression stiffness,  $E_{oed}$ , on the ground deformations observed. The  $E_{oed}$  parameter is related to the isotropic compression stiffness. The results demonstrate that larger displacements at the ground surface, compared to those at depth, occur when the 1D-compression stiffness ( $E_{oed}$ ) is significantly smaller than the secant stiffness at 50% of failure,  $E_{50}$ . This is a consequence of the pronounced increase in volumetric contractive strains near the ground surface above the tunnel as  $E_{oed}$  decreases. Observing larger settlements at the surface than at depth is an unusual behavior commonly seen in tunnels excavated in porous clays. Thus, the results presented in this paper suggest that the Hardening Soil Model can represent this unusual behavior by selecting an  $E_{oed}$  that is sufficiently smaller than  $E_{50}$ .

**KEYWORDS:** Shallow tunnel, Hardening Soil Model, Numerical modeling, FEM, Compressible soils, Collapsible Soils, Porous clay.

## 1 INTRODUCTION

Tunneling in compressible soils can lead to substantial surface displacements that can damage the nearby infrastructure. These soils undergo significant contractile volumetric deformations, resulting in a complex distribution of displacements around the tunnel. High void ratios and unsaturated conditions often characterize the porous clays. Notable examples of tunneling in such conditions include the Metro tunnels in Brasília (Ortigão et al., 1996; Marques, 2006) and the Paraíso tunnel in São Paulo (Parreira, 1991; Azevedo et al, 2002; Almeida e Souza et al., 2011; Vitali et al., 2022a). In these tunnels, the settlements at the surface were often greater than those at depth, which is an unusual behavior.

The complex behavior of these soils presents challenges in predicting their response. Marques (2006) and Almeida e Souza et al. (2011) modeled the Brasília and Paraíso tunnels, respectively, using the finite

element method. They employed the Lade's constitutive model (Lade, 1977) to capture soil behavior, which requires 16 input parameters and as well as a rigorous parameter calibration process. In contrast, Vitali et al. (2022) achieved excellent agreement between the 3D FEM modeling and tunnel instrumentation data for the Paraíso tunnel using the well-known Hardening Soil Model (Schanz et al., 1999). The Hardening Soil Model combines simplicity with efficiency, incorporating features from other constitutive models. It adopts the hyperbolic stress-strain relationship for drained triaxial tests as proposed by Duncan and Chang (1970) and integrates the hardening mechanism due to increased confining stress observed in oedometer tests, originally formulated by the Cam-Clay model (Schofield and Wroth, 1968). Additionally, unloading is assumed to be linear-elastic, with stiffness varying as an exponential function of the minor principal stress. The failure criterion it uses is the Mohr-Coulomb envelope.

In this study, a 2D plane-strain FEM model was developed to analyze the Paraíso tunnel, employing the Volume Loss Control technique (Addenbrooke et al., 1999). The Hardening Soil Model parameters calibrated by Vitali et al. (2022a) were adopted. A good match between numerical results and field data was achieved for a tunnel volume loss of 1.25%. Subsequently, a sensitivity analysis was performed, varying the 1D compression stiffness,  $E_{oed}$ , which is related to the isotropic compressive behavior of the soil. The objective of the parametric analysis was to assess the ability of the Hardening Soil Model to replicate the unusual behavior of shallow tunnels excavated in porous clays.

## 2 SOIL BEHAVIOR AND FEM MODELING

The Paraíso Tunnel, situated in São Paulo, was completed in 1991 and is detailed in Parreira (1991). This tunnel was excavated in the well-known red residual porous clay of São Paulo (Massad et al., 1992). Parreira (1991) conducted an extensive series of laboratory tests on this soil using undisturbed samples extracted at depths of 3.5 and 6.5 meters. These tests were selected by Vitali et al. (2022a) to calibrate the hardening soil model.

Table 1 illustrates the parameters of the Hardening Soil Model calibrated by Vitali et al. (2022a) alongside the  $E_{oed}$  values utilized in the sensitivity analysis. The 1D compression stiffness (or oedometer stiffness) correlates with the plastic deformations induced by increased soil confinement. Typically, the 1D compression stiffness approximates the secant stiffness in drained triaxial tests. Notably, to capture the compressible behavior of the red residual porous clay, Vitali et al. (2022a) adopted a relationship  $E_{oed}=E_{50}/3$ .

Figure 1 presents the results of triaxial compression tests conducted by Parreira (1991) under confining stress of 50 kPa. Just one confinement stress is sufficient to illustrate the response of  $E_{oed}$  in soil behavior. Figure 1 plots the deviatoric stress ( $q$ ) and volumetric strain ( $\varepsilon_{vol}$ ) against axial strain ( $\varepsilon_{ax}$ ). The numerical results for different  $E_{oed}$  are depicted. The base case ( $E_{oed}=E_{50}/3$ ) closely aligns with the experimental data, which was calibrated by Vitali et al. (2022a). When considering  $E_{oed}=E_{50}$ , the contractile volumetric variations decrease significantly, albeit without a substantial stiffness gain. In the case of  $E_{oed}=E_{50}/12$ , the contractile volumetric variations become pronounced, and the soil exhibits a significant loss of stiffness, indicating a substantially more compressible behavior.

Figure 2 shows the 2D plane strain finite element mesh with second order elements (quadratic shape function) adopted to represent the Paraíso tunnel. Boundary conditions and mesh refinement followed the recommendations from Vitali et al. (2018a, 2021a) and Vitali et al., 2024. These recommendations have been validated by matching exact analytical solutions (Vitali et al., 2018b; 2019a; 2019b; 2019d; 2020a; 2020b; 2020c; 2021b; 2022b) and by replicating the observed behavior of underground excavations (Vitali et al., 2019c; 2022a). At approximately the springline of the tunnel, a division occurs between the porous clay layer and the stiff clay layer. The stiff clay was modeled using a perfect elastoplastic model, with elastic parameters defined as 120 MPa for the Young Modulus and 0.17 for Poisson's ratio, following the Mohr-Coulomb failure criterion ( $c=66$  kPa and  $\phi=25^\circ$ ). Those are the same parameters adopted in previous studies (Almeida e Souza et al., 2011).

The modeling process was conducted in two steps. Initially, the stress state was generated according to the  $K_0$  condition, with a natural specific weight of 15 kN/m<sup>3</sup> and  $K_0=0.5$  for the porous clay, and a natural specific weight of 18 kN/m<sup>3</sup> and  $K_0=0.84$  for the stiff clay. Displacements from this step were disregarded. Subsequently, stress relief was implemented. Nodal forces replaced the finite element mesh representing the excavated volume to achieve equilibrium. These forces were gradually reduced until a specified tunnel volume

loss was attained. The tunnel volume loss is expressed as a percentage, calculated by the ratio of the volume loss due to tunnel displacements and the initially excavated volume. This procedure is described by Addenbroke et al. (1999) and adopted by Vitali et al. (-) and Vitali (-) to successfully replicate centrifuge tunnel tests.

Table 1. Hardening Soil Model Parameters.

Parameter	Definition	Value
$E_{50,ref}$ (kPa)	Secant stiffness in standard drained triaxial test	6000
		500 (= $E_{50,ref} / 12$ )
$E_{oed,ref}$ (kPa)	Tangent stiffness for primary oedometer loading	2000 for base case
		6000 (= $E_{50,ref}$ )
$E_{ur,ref}$ (kPa)	Unloading / reloading stiffness	12000
$R_f$	Failure ratio	0.9
$p_{ref}$ (kPa)	Reference stress for stiffness	50
$m$	Power for stress-level dependency of stiffness	1
$\phi$ (°)	Angle of internal friction	30
$K_{0,NC}$	$K_0$ -value for normal consolidation	0.5
$\Psi$ (°)	Angle of dilatancy	0
$c$ (kPa)	Cohesion	30
$\gamma_n$ (kN/m <sup>3</sup> )	Natural specific weight	15
$\nu$	Poisson's ratio for unloading-reloading	0.27
OCR	Overconsolidation ratio	1

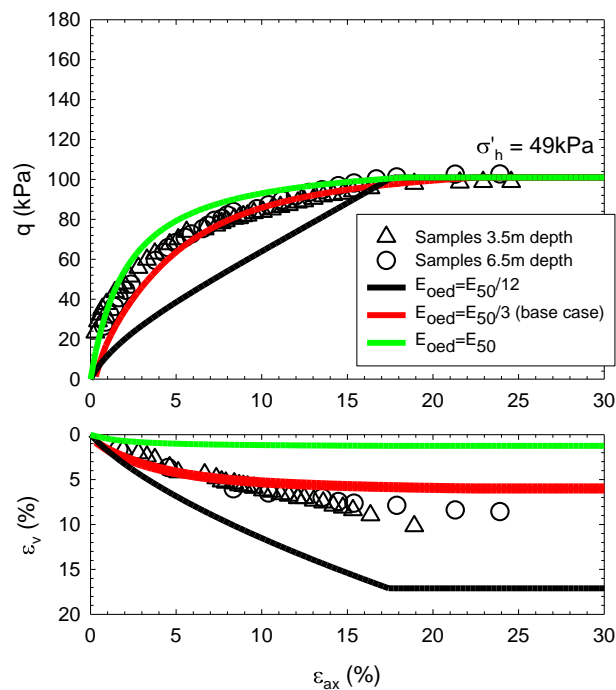


Figure 1. Experimental data and numerical simulations of the triaxial compression tests under 50 kPa confinement stress.

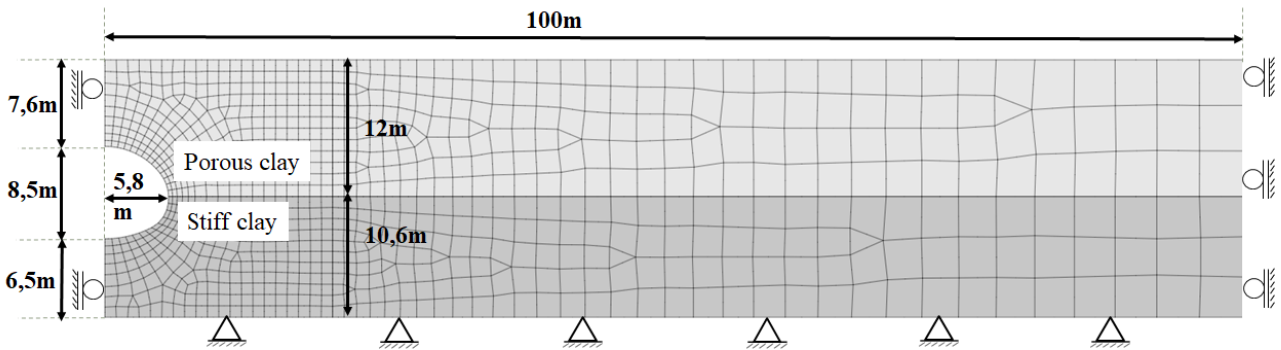


Figure 2. Plane strain finite element mesh for the Paraiso Tunnel.

### 3 RESULTS AND DISCUSSION

Employing the Volume Loss Control technique and using the calibrated Hardening Soil Model parameters to analyze the Paraiso tunnel, we found that a tunnel volume loss of 1.25% resulted in a good alignment between the numerical results and field data. Note that the tunnel volume loss, derived from displacements at the tunnel perimeter, differs from the soil volume loss, which is measured from the settlement trough. In this case, the soil volume loss is substantially larger than the tunnel volume loss due to significant soil contraction.

Figure 3 illustrates the settlement trough measured during the tunnel's construction (field data) alongside the numerical results for a tunnel volume loss of 1.25%. The base case, which uses the calibrated Hardening Soil Model parameters with  $E_{50}=3E_{oed}$ , predicts the shape of the settlement trough reasonably well. It is noteworthy that the magnitude and shape of the settlement trough vary significantly with changes in the 1D compression stiffness ( $E_{oed}$ ), even when the tunnel volume loss remains the same. Specifically, when  $E_{50}$  equals  $E_{oed}$ , the model predicts smaller displacements and narrower settlement troughs. Conversely, a more compressible soil condition ( $E_{oed} = E_{50}/12$ ) results in larger displacements and wider settlement troughs.

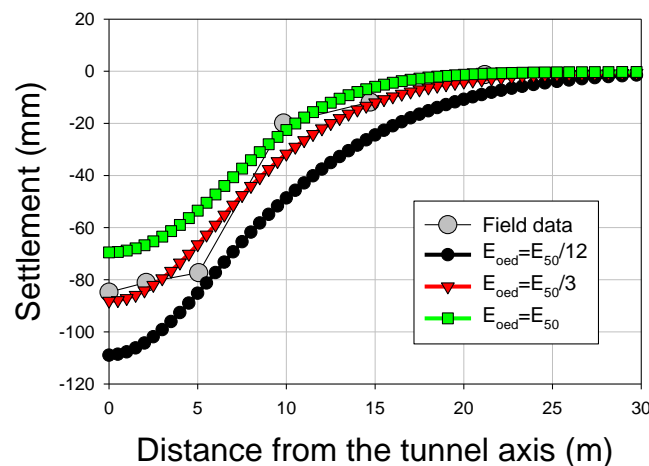


Figure 3. Settlement troughs from field data and 2D plane-strain FEM simulations.

Figure 4 shows the vertical displacements at depth above the tunnel crown. Field data and studied numerical cases are shown. The base case replicates well the field data, where vertical displacements were relatively constant with depth. With  $E_{oed}=E_{50}/12$ , surface displacements were larger than those at depth, whereas for  $E_{50}=E_{oed}$  the opposite was observed. For shallow tunnels in porous clays, it is often observed that settlements at the ground surface are larger than those at depth. This outcome is highly unusual, as vertical displacements normally increase with depth in shallow tunnels (Mair et al., 1993). The results presented indicate that this uncommon behavior can be simulated using the Hardening Soil Model by adopting a

substantially smaller  $E_{oed}$  with respect to  $E_{50}$ . França (2006), to the best of our knowledge, was the first to point out this characteristic of the Hardening Soil Model.

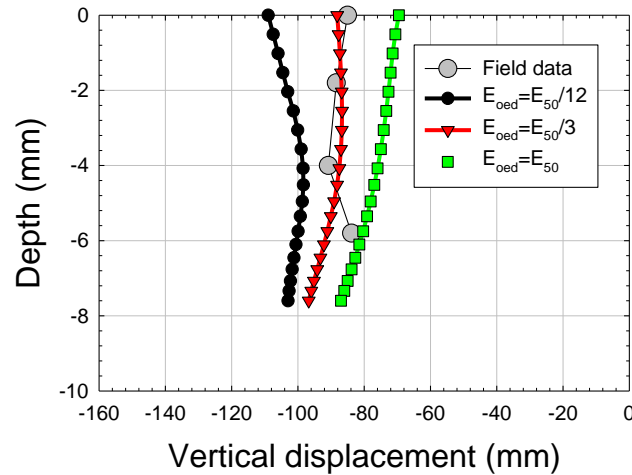


Figure 4. Vertical displacements with depth above the tunnel crown from field data and numerical simulations.

Figure 5 depicts tunnel deformations when the tunnel volume loss ( $V_{Lt}$ ) is equal to 1.25%. Displacements have been amplified by 10 times. In all cases, the part of the tunnel in stiff clay practically remained undeformed. In line with Figure 4, the case where  $E_{oed}=E_{50}/12$  showed greater displacements at the tunnel crown. Conversely,  $E_{oed}=E_{50}$  exhibits greater displacements at the tunnel springline. Therefore, higher stiffness seems to result in more evenly distributed displacements around the tunnel.

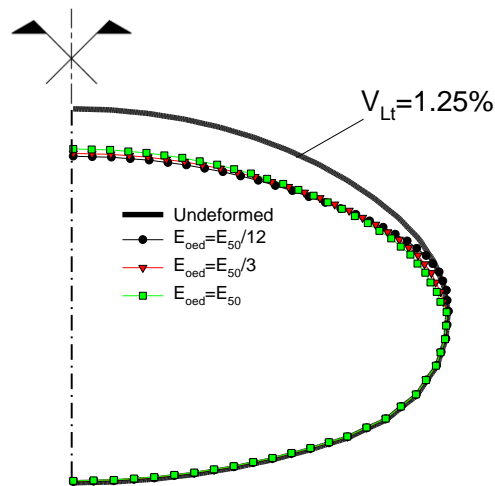
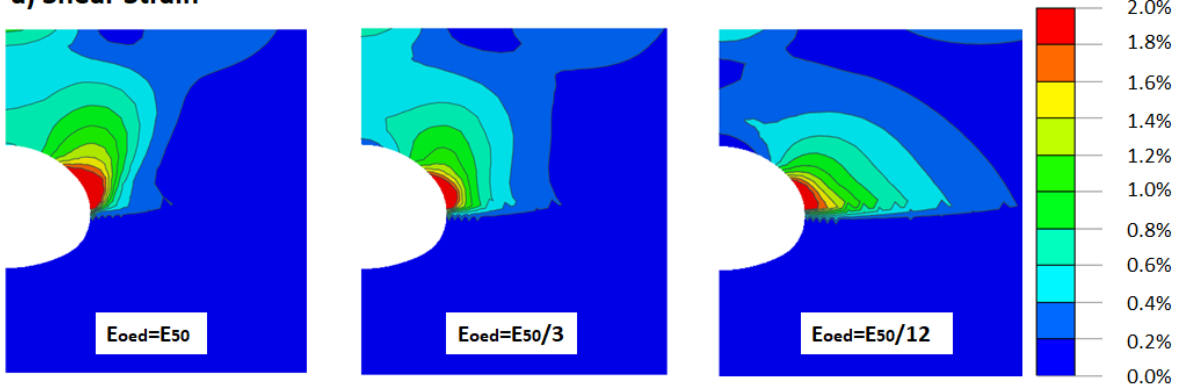


Figure 5. Tunnel-deformed shape for the different cases.

Figure 6 illustrates the maximum shear and volumetric strain fields for the three cases studied for a tunnel volume loss of 1.25%. From the figure, it is evident that stiffer soils mobilize more pronounced shear strains to achieve the same tunnel volume loss, as expected. However, contractile volumetric deformations are substantially more pronounced in soils with smaller  $E_{oed}$  for a given  $E_{50}$ . Notably, in all cases, the volumetric contraction at the ground surface above the tunnel was larger than that at the tunnel crown. For an  $E_{50}/E_{oed}$  ratio of 1/12, the soil contraction near the ground surface was significantly greater than for a ratio of 1, while the soil contraction near the tunnel crown was only marginally larger for a ratio of 1/12 compared to 1. This mechanism explains the larger displacements observed at the ground surface, compared to those at depth, as the  $E_{oed}$  decreases. Additionally, shear and volumetric contraction strains develop over larger areas as the soil compressibility increases. Therefore, tunnels in compressible soils induce greater displacements over a larger area, a factor that should be taken into consideration in assessments of damage to adjacent structures.



**a) Shear Strain**



**b) Volumetric Strain**

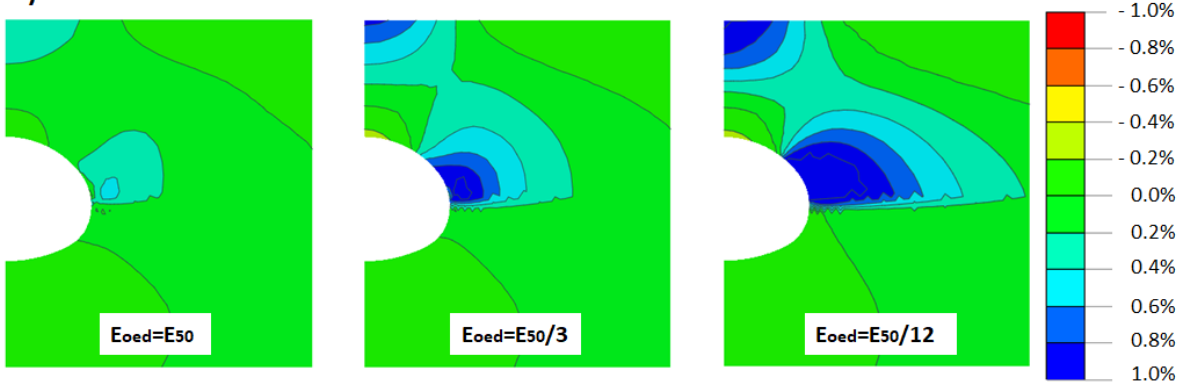


Figure 6. Shear strain fields (a) and volumetric strain fields (b).

#### 4 CONCLUSION

In this study, the Paraíso tunnel was analyzed using 2D-plane strain Finite Element Method (FEM) modeling and the volume loss control technique, employing the well-known Hardening Soil Model. This tunnel was excavated in porous clay, characterized by its highly compressible behavior and unsaturated conditions. The parameters for the Hardening Soil Model were calibrated by Vitali et al. (2022a) based on triaxial tests conducted by Parreira (1991) on undisturbed samples of the same residual porous clay. From this calibration, it was determined that the ratio between the 1D-compression stiffness (or oedometer stiffness,  $E_{oed}$ ) and the secant stiffness at 50% to failure ( $E_{50}$ ) is  $E_{50}/E_{oed} = 3$ . This ratio is notable since, for most soils, this value is expected to be close to 1. However, considering the highly compressible and unusual behavior of São Paulo's porous clay, this ratio is deemed reasonable.

The settlements at the ground surface predicted by the 2D-plane strain numerical model, using the calibrated Hardening Soil Model with  $E_{50}/E_{oed}=3$  and the tunnel volume loss control technique, matched the displacements measured during the tunnel's construction for a tunnel volume loss of 1.25%. Following that, the impact of the 1D-compression stiffness,  $E_{oed}$ , on induced ground deformations was assessed. The analysis considered a softer 1D-compression stiffness ( $E_{oed}=E_{50}/12$ ) and a typical  $E_{oed}$  value for most soils ( $E_{oed}=E_{50}$ ).

The findings indicate that volumetric contractive strains near the ground surface above the tunnel significantly increase as  $E_{oed}$  decreases. In contrast, near the tunnel crown, the soil contraction is only slightly affected by  $E_{oed}$ . Consequently, the smaller the  $E_{oed}$  is relative to a given  $E_{50}$ , the greater the settlement at the ground surface compared to the settlement at depth near the tunnel crown.

Larger surface displacements compared to those at depth represent an unusual behavior, often observed in shallow tunnels in porous clayey soils. Therefore, these results suggest that the behavior of porous clays can be represented by adopting a relatively small  $E_{oed}$  with respect to  $E_{50}$ . This has significant practical implications because the Hardening Soil Model is a well-established constitutive model in geotechnical engineering practice, and  $E_{oed}$  and  $E_{50}$  values can be readily obtained from laboratory tests or estimated from in-situ testing.

## ACKNOWLEDGMENTS

The authors acknowledge the support provided by the research funding agency of the Brazilian Government, CNPq (Conselho Nacional de Desenvolvimento Científico e Tecnológico), Contract 162113/2020-0: Post-Doctoral Scholarship, and CAPES (Coordenação de Aperfeiçoamento de Pessoal de Nível Superior). The authors also thank Midas Technology Information Co. Ltd. for providing the license for the Midas GTS NX software utilized in this research.

## REFERENCES

- Addenbrooke T. I., Potts D. M. and Puzrin A. M. (1997). *The influence of pre-failure soil stiffness on the numerical analysis of tunnel construction*. Géotechnique 47, No. 3, 693–712.
- Almeida e Sousa, J., Negro, A., Matos Fernandes, M., & Cardoso, A. S. (2011). *Three-Dimensional Nonlinear Analyses of a Metro Tunnel in São Paulo Porous Clay, Brazil*. Journal of Geotechnical and Geoenvironmental Engineering, 137(4), 376–384.
- Azevedo, R. F., Parreira, A., & Zornberg, J. G. (2002). *Numerical analysis of a tunnel in residual soils*. Journal of Geotechnical and Geoenvironmental Engineering, 128(3), 227–236.
- Duncan, J.M., Chang, C.Y. (1970). *Nonlinear analysis of stress and strain in soil*. ASCE J. of the Soil Mech. And Found. Div., 96, 1629–1653.
- França P.T. (2006). *Study of the behaviour of tunnels: elasto-plastic constitutive model three-dimensional numerical analyses (in portuguese)*. Master's dissertation. University of São Paulo
- Lade, P. V. (1977). *Elasto-plastic stress-strain theory for cohesionless soil with curved yield surfaces*. International journal of solids and structures, 13(11), 1019-1035.
- Massad, F., Pinto, C. de S., & Nader, J. J. (1992). *Strength and Deformability*. Brazilian Society of Soil Mechanics Conference on Soils of the São Paulo city, 141–179 (in Portuguese).
- Marques, F. E. R. (2006). *Behavior of Shallow Tunnels in Porous Soils – the Brazilia Metro Case* [Doctoral dissertation]. University of Coimbra (in Portuguese).
- Mair, R. J., Taylor, R. N. and Bracegirdle, A. (1993). *Subsurface settlement profiles above tunnels in clay*. Géotechnique 43, No. 2, 315–320, <https://doi.org/10.1680/geot.1993.43.2.315>.
- Ortigão, J. A. R., Kochen, R., Farias, M. M., & Assis, A. P. (1996). *Tunnelling in Brasilia porous clay*. Canadian Geotechnical Journal, 33 (4), 565–573.
- Parreira, A. B. (1991). *Analysis of shallow tunnels in soil. The NATM Paraíso Tunnel at Paulista Avenue in São Paulo City* [Doctoral dissertation]. Catholic University of Rio de Janeiro, Rio de Janeiro, Brazil (in Portuguese).
- Schanz, T., Vermeer, P. A., & Bonnier, P. G. (1999). *The hardening soil model: Formulation and verification*. In Ronald B. J. Brinkgreve (Eds.), *Beyond 2000 in Computational Geotechnics* (pp.281–296). Routledge.
- Schofield, A. N., & Wroth, P. (1968). *Critical state soil mechanics* (Vol. 310). London: McGraw-hill.
- Vitali, F. P. M; (2024). *Deformations caused by tunnel excavation in sandy ground (in portuguese)*. Master's dissertation. São Carlos School of Engineering, University of São Paulo. In preparation.
- Vitali, F. P. M; Vitali, O. P. M.; Celestino T. B.; Bobet, A. (2024) *FEM modeling requirements for accurate highly nonlinear shallow tunnels analysis*. Soil and Rocks. 47(1). 10.28927/SR.2024.000923.
- Vitali, F. P. M; Vitali, O. P. M.; Celestino T. B.; Bobet, A. (-) *Impact of Relative Density on Shallow TBM Tunnel Excavation: Ground Behavior and Building Damage Risks*. In review.
- Vitali, O. P. M., Celestino, T. B., & Bobet, A. (2018a). *3D finite element modeling optimization for deep tunnels with material nonlinearity*. Undergr. Sp., 3(2):125–139. <https://doi.org/10.1016/j.undsp.2017.11.002>

- Vitali, O.P.M., Celestino, T.B., & Bobet, A., (2018b). *Analytical solution for tunnels not aligned with geostatic principal stress directions*. *Tunn. Undergr. Sp. Technol.* 82, 394–405. <https://doi.org/10.1016/j.tust.2018.08.046>.
- Vitali, O. P. M., Celestino, T. B., & Bobet, A. (2019a) *Shallow tunnel not aligned with the geostatic principal stress directions*. In: *Proceedings of Geo-Congress2019, GSP*, 313:214-222. <https://doi.org/10.1061/9780784482155.023>
- Vitali, O. P. M., Celestino, T. B., & Bobet, A. (2019b) *Shallow tunnels misaligned with geostatic principal stress directions: analytical solution and 3D face effects*. *Tunn. Undergr. Sp. Technol.*, 89: 268-283. <https://doi.org/10.1016/j.tust.2019.04.006>
- Vitali, O.P.M., Celestino, T.B., & Bobet, A., (2019c). *Progressive failure due to tunnel misalignment with geostatic principal stresses*. In: *Proceedings of ISRM 14th International Congress on Rock Mechanics*, pp. 2292-2299.
- Vitali, O. P. M., Celestino, T. B., & Bobet, A. (2019d). *Buoyancy effect on shallow tunnels*. *International Journal of Rock Mechanics and Mining Sciences*, 114, 1–6. <https://doi.org/10.1016/j.ijrmmms.2018.12.012>
- Vitali, O.P.M., Celestino, T.B., & Bobet, A., (2020a). *Analytical solution for a deep circular tunnel in anisotropic ground and anisotropic geostatic stresses*. *Rock Mech. Rock Eng.* 53 (9), 3859–3884. <https://doi.org/10.1007/s00603-020-02157-5>
- Vitali, O.P.M., Celestino, T.B., & Bobet, A., (2020b). *Tunnel misalignment with geostatic principal stress directions in anisotropic rock masses*. *Soils and Rocks*, São Paulo, 43(1), 123-138, January-March, 2020, <https://doi.org/10.28927/SR.431123>.
- Vitali, O.P.M., Celestino, T.B., & Bobet, A., (2020c). *Deformation patterns and 3D face effects of tunnels misaligned with the geostatic principal stresses in isotropic and anisotropic rock masses*. *54th US Rock Mechanics /Geomechanics Symposium (ARMA 2020)*.
- Vitali, O. P. M., Celestino, T. B., & Bobet, A. (2021a). *New modeling approach for tunnels under complex ground and loading conditions*. *Soils and Rocks* 44 (1), 1–8. <https://doi.org/10.28927/SR.2021.052120>.
- Vitali, O.P.M., Celestino, T.B., Bobet, A., (2021b). *Behavior of tunnels excavated with dip and against dip*. *Underground Space* 6 (6), 709–717. <https://doi.org/10.1016/j.undsp.2021.04.001>.
- Vitali, O. P. M., Celestino, T. B., & Bobet, A. (2022a). *Construction strategies for a NATM tunnel in São Paulo, Brazil, in residual soil*. *Underground Space*, 7(1):1-18. <https://doi.org/10.1016/j.undsp.2021.04.002>.
- Vitali, O. P. M., Celestino, T. B., & Bobet, A. (2022b). *3D face effects of tunnels misaligned with the principal directions of material and stress anisotropy*. *Tunnelling and Underground Space Technology*, 122, 104347. <https://doi.org/10.1016/j.tust.2021.104347>